J Food Sci Technol (December 2015) 52(12):7964–7973
DOI 10.1007/s13197-015-1939-4

ORIGINAL ARTICLE

Serish inulin and wheat biopolymers interactions in model systems as a basis for understanding the impact of inulin on bread properties: a FTIR investigation

Amir Pourfarzad[1] · **Mohammad B. Habibi Najafi**[2] · **Mohammad H. Haddad Khodaparast**[2] · **Mohammad Hassanzadeh Khayyat**[3]

Revised: 7 June 2015 / Accepted: 2 July 2015 / Published online: 22 July 2015

Abstract In this study the interactions between Serish root inulin and the main biopolymer types of wheat flour namely gluten, starch and phospholipid, were investigated in different model systems using Fourier transform infrared (FTIR) spectroscopy to unravel the underlying physical mechanism by which inulin impacts dough and bread properties. Interactions of inulin with starch and phospholipid were not considerable compared to gluten, but it was also clear that the modes of these interactions varied with the type and the amount of additives used in model formulation. This study revealed that when inulin is added to gluten, water redistribution promotes partial dehydration of gluten and collapse of β-spirals into intermolecular β-sheet structures; this trans-conformations might be due to physical reasons are believed to further impact the poor quality of bread containing added inulin. Upon performing Gaussian–Lorenzian curve fitting, it was observed that by adding of inulin to model systems, the relative contribution of characteristic peaks of β-turn and intramolecular β-sheet was progressively decreased whereas intermolecular β-sheet and α-helix contents were increased.

Keywords Wheat flour component interactions · Fourier-transform infrared spectroscopy · Gluten secondary structure · Serish root inulin

Research Highlights • A novel resource for inulin isolation was developed.
• Understanding the interactions between added inulin and typical bread ingredients.
• FTIR was used for studying interactions among inulin and bread components.
• Investigation of the gluten secondary structure by second-derivative transformation.

✉ Amir Pourfarzad
amir.pourfarzad@gmail.com

[1] Department of Food Science and Technology, Faculty of Agricultural Sciences, University of Guilan, RashtP.O. Box 41635-1314, Iran

[2] Department of Food Science and Technology, Ferdowsi University of Mashhad, Mashhad, Iran

[3] Pharmaceutical Research Center, Department of Medicinal Chemistry, School of Pharmacy, Mashhad University of Medical Sciences, Mashhad, Iran

Introduction

There has been increasing demand for food products with additional health benefits including reduction of risk of colonic diseases, noninsulin-dependent diabetes, obesity, osteoporosis and cancer (Roberfroid 1999). In this respect, the enrichment of wheat bread with the functional components such as inulin, is considered an interesting subject to both the consumer as well as the cereal industry, since wheat bread is considered as an important staple food in the world (Peressini and Sensidoni 2009).

Inulin as a natural component of several edible fruits and vegetables, is a mixture of molecules consisting of fructose moieties linked to each other by β (2→1) bonds. Inulin-type fructans are known to exert many food and pharmaceutical applications and are widely used in functional foods throughout the world for their nutritional and techno-functional properties (O'brien et al. 2003).

Serish (*Eremurus spectabilis*) belongs to the family of Liliaceae and geographically distributed in the area of South and Central Asia, including Iran, West Pakistan, Afghanistan, Iraq, Turkey, Palestine, Lebanon, Syria and Caucasus. Its roots accumulate high levels of fructans during their growth and thus it could be used as a new resource of inulin (Pourfarzad et al. 2015a).

Food is composed of molecular dispersions of biopolymers and their complexes. The major biopolymers in wheat flour, protein and starch, are fundamental to the structure, rheology, and other physical properties of breads, as well as their taste and sensory perception. Water and lipids, binding to other components or acting as solvents, are important factors as well. In the case of bread, it had already been reported that its properties changed compared to the individual components. As such, the functional properties of bread reflect the physico-chemical properties of both the complex network and the individual macromolecules. In this way, interactions between macromolecules contribute to the diversity of bread structures. During dough mixing, the mechanical energy communicated makes conformational changes in wheat proteins, such as breakage and formation of both covalent and non-covalent bonds e.g., hydrophobic and H bonds (Aït Kaddour et al. 2008). Baking involves heat and mass transfer, causing thermally induced protein structural changes and/or denaturation, as well as increased cross-linking and polymerization of gluten polymers due to increased sulphydryl (SH) and disulphide (SS) interchange reactions (Tiwari et al. 2011). Interactions take place between gelatinized starch granules and the gluten network through hydrogen bonding interactions during baking. Although, lipids and in particular phospholipids, are present in small quantities in wheat, they have a significant effect on the final texture of wheat containing food products. As indicated in the literature reports, polar lipids, i.e., phospholipids and glycolipids interact primarily with wheat gluten protein (Sivam et al. 2012).

FTIR spectroscopy identifies specific functional groups within a molecule based on absorption bands at characteristic frequencies. It is a well-established tool in the determination of chemical composition and molecular structure of heterogeneous foods and biological materials and can provide valuable information in the development process of ideal formulations and process parameters (Vonhoff et al. 2010). IR spectroscopy is based on the changes in the electrical dipole moment of chemical bonds, and thus yields different vibrational spectroscopic information. FTIR spectroscopy can be used to analyze the secondary structures and conformations of protein/polysaccharides based on the characteristic absorption bands of specific functional groups contained within these biopolymers such as the amide I band of proteins at 1600–1700 cm^{-1} and the bands of carbohydrates at the region 1200–950 cm^{-1} (Sivam et al. 2012).

Previous studies showed that inulin addition significantly influences the properties of bread dough and subsequently bread (Peressini and Sensidoni 2009). To our knowledge, no reports have been found on the investigation of the interactions between added inulin and typical bread ingredients, which may then lead to the development of novel and improved functional breads. Thus, the present study is considered the first attempt aiming: (a) to explore the conformational changes of systems containing Serish inulin and wheat biopolymers (gluten, starch and phospholipids) in model systems using FT-IR technique; (b) to investigate the secondary structure changes of gluten caused by other wheat biopolymers and inulin using second-derivative transformation and Gaussian–Lorenzian curve fitting.

Materials and methods

Materials

The Serish root powders were obtained from the local medical plant market, Mashhad, Iran. Wheat gluten (catalog number G-5004, ≥80 % protein), soybean L-α-lysophosphatidylcholine (catalog number 62963, ≥98 % phospholipid), and wheat starch (catalog number G-5004, ≥98 % starch) were purchased from Sigma–Aldrich (Gillingham, Dorset, UK). All other chemicals, reagents and solvents were of analytical grade.

Methodology

Preparation of Serish inulin

Inulin extraction was carried out in a water bath (model WB/0B7-45, Memmert Company, Schwabach, Germany). Serish root powder was suspended in distilled water at a ratio of 1:50 (*w/v*) and was allowed to stand at 85–90 °C for 30 min under agitation (Pourfarzad et al. 2015a). The suspension was then filtered through muslin cloth to remove the insoluble residues. The resulting solution was turbid due to the presence of particulate and colloidal matter, i.e., pectin, protein, and cell wall substances. To remove these impurities, the concentrate was mixed with 5 % slurry of calcium hydroxide and incubated at 50–60 °C for 30 min, resulting in the formation of a flocculent precipitate and a brighter yellow supernatant. By this technique, the pH of solution was increased from 5–6 to 10–12. After filtration under vacuum using paper filter (Whatman No. 4), 10 % phosphoric acid was added to the filtrate with vigorous stirring to adjust its pH to 8–9, causing the precipitation of surplus calcium and coagulated organic material. The mixture was permitted to stand at 60 °C for 2–3 h before re-filtration (Whatman No. 4). The clarification process was repeated twice. Activated carbon powder was added to the filtrates at 60 °C and mixed for 15–30 min to facilitate elimination of coloring materials. The treated solution was filtered (Whatman No. 1) and the clear achieved solution was further concentrated by rotary evaporation at 70 °C. The concentrated inulin solution with soluble solids level of 40 °Brix which was obtained after the evaporation process, was mixed with 8.5 parts by weight of ethanol (abs. 99 %) and stored at 20–25 °C for 3 days (Pourfarzad et al. 2014). After storage, the

supernatants were removed and the precipitates washed with ethanol. Precipitated Serish inulin was frozen at −20 °C for 24 h followed by drying at −30 °C in a freeze dryer (Martin christ, 8891, type 317, Germany) for 24 h (Pourfarzad et al. 2015b). The dried inulin was dry milled and passed through a 1.0 mm mesh sieve and packed in the air-tight containers prior to further spectroscopic analyzes. The purity and degree of polymerization of produced inulin, which were determined with methods described by Pourfarzad et al. (2014), were 93.8 % and 13, respectively.

Model systems preparation

The compositions of model systems consisting of inulin, starch, gluten and phospholipid investigated in this study are given in Table 1. The weight ratios of components in models were selected according to the their ratio in the wheat flour. Level of inulin addition in models 18–24 was 10 % of total amount of other components according to the literature (Morris and Morris 2012). The weight ratio of water to total solids content (i.e., inulin + starch + gluten + phospholipid) in the blends was 3:1. First, the blends were dispersed in distilled water under continuous agitation. Then the dispersions were held at 30 °C for 16 h to allow the components of model systems to interact completely with each other (Mohamed et al. 2009). The resulting blends were freeze-dried and pulverized under liquid nitrogen to give fine powders that were used to obtain the test spectra. It should be indicated that moisture content of prepared models after freeze-drying was about 6.5 %. As shown in Table 1, inulin, starch, gluten and phospholipid were each treated separately, as mentioned above, to prepare control spectra of the components alone.

Table 1 Variables and weight ratios used in model systems

trial	inulin	gluten	starch	phospholipid
1	1	0	0	0
2	0	1	0	0
3	0	0	1	0
4	0	0	0	1
5	1	0.5	0	0
6	1	1	0	0
7	1	1.5	0	0
8	1	2	0	0
9	1	0	0.5	0
10	1	0	1	0
11	1	0	1.5	0
12	1	0	2	0
13	1	0	0	0.5
14	1	0	0	1
15	1	0	0	1.5
16	1	0	0	2
17	0	1	7	0
18	0.8	1	7	0
19	0	1	0	0.2
20	0.12	1	0	0.2
21	0	1	7	0.2
22	0.82	1	7	0.2

The weight ratios of components in models were selected according to the their ratio in the wheat flour; Level of inulin addition was 10 % of total amount of other components according to the literature

FT-IR analysis

Fourier-transform infrared spectroscopic (FT-IR) studies were performed in transmission mode on a spectrophotometer (Paragon 1000, Perkin Elmer, USA). Samples were blended with KBr powder, and pressed to form a tablets before measurement. Spectra were obtained at 4 cm^{-1} of resolution from 4000 to 400 cm^{-1}. The interference of water and CO_2 from air was deducted during scanning (Panchev et al. 2011).

Direct comparisons of spectral changes were done on vector normalized second derivatives of average spectra of the discussed spectral classes, because most IR absorption bands are broad and composed of overlapping components. Second derivative resolution enhancement were used to narrow the width of infrared bands and increase the separation of the overlapping components with Unscrambler v. 9.2 software (Camo process AS, Oslo, Norway). The resolution enhancement resulting from the second derivative was such that the number and the position of the bands to be fitted were readily determined. In experiments involving inulin, starch and phospholipid addition, the spectrum of them was subtracted from the gluten spectrum. At first, normalized spectra were subjected to a multipoint linear base-line correction using the Unscrambler software. The spectra were then curve fitted with Gaussian–Lorenzian mix function for the amide I band region (1600–1700 cm^{-1}). The iterative data fitting was performed until a satisfactory 'goodness of fit' was achieved. The relative peak areas (RPAs) of the absorbance bands were expressed as "percentage of the area of fitted region" (Byler and Susi 1986; Sivam et al. 2012).

Statistical analyses

Results given as the average of three replications (all treatments were evaluated in three batches). In order to assess the significant differences among different interactions, a complete randomized design of triplicate analyzes of samples was performed using the Minitab 15 (Minitab Inc., State College, PA, USA) software. Duncan's new multiple range tests were used to study the statistical differences of the means with 95 % confidence.

Results and discussion

FT-IR spectra for ingredients

FT-IR absorbance spectra for the models ingredients are presented in Figs. 1, 2 and 3. In this study, all ingredients showed bands at 2800–3000 cm^{-1} and a broad feature at ~3300 cm^{-1}, due to C—H stretching modes and intermolecular H-bonded and O—H stretching modes respectively (Nikolic and Cakic 2007). The gluten spectrum had peaks centered at 2934 and 3397 cm^{-1} region (CH, and NH or OH stretching modes, respectively). For starch and inulin, additional features are observed around 800–1200 cm^{-1} which are characteristic for polysaccharides. The characteristic bands of starch are at 1010, 1080 and 1150 cm^{-1}, which are associated with the coupled C—O and C—C stretching vibrations of the polysaccharide molecules. In the inulin spectrum, the absorbance around 600–800 cm^{-1} reflected the absorption of the C-H aliphatic bending. The relatively strong absorption peak at around 1653 cm^{-1} reflected the absorption of the OH bending signal of adsorbed water (Pal et al. 2005). On the other hand, C–C stretching vibrations were observed at 1100–1200 cm^{-1} in the spectrum of phospholipid. Other peaks are assigned to C-H bond (724 and 1460 cm^{-1}) and C=O stretching (1745 cm^{-1}) vibrations. The spectra are basically similar to the previously analyzed spectra of other examined systems (Sivam et al. 2012).

It should be mentioned that the direct comparisons of spectral changes were done on vector normalized spectra. The discussion on the results were done basis on the normalized spectra. The complexity of normalized spectra led to an unclear view. Thus, spectra shifting were used in order to resolution and best evaluation of them. This process resulted in some changes in the displaying of their intensity.

Inulin - starch interaction

Infrared spectra of starch and inulin exhibited complex vibrational modes at low wavenumbers (below 800 cm^{-1}) due to the skeletal mode vibrations of the fructose and glucose pyranose rings (Kizil et al. 2002). In this study, major bands at 760 and 577 cm^{-1} and minor bands between 577 and 400 cm^{-1} in the infrared spectra (Fig. 1) of starch and inulin were attributed to the skeletal modes of the pyranose ring. The enhancement of intensity at this wavenumbers is related to increasing levels of starch and inulin in the models. The intensity of peaks at 862 and 805 cm^{-1}, which were significantly originated from the CH out-of -plane deformations of starch and inulin molecules (Tipson 1968), increased with increasing of starch and inulin levels in the system models. The region of 1300–900 cm^{-1} (C-C and C-O) in the IR spectrum is sensitive to the conformation of carbohydrates (Goodfellow and Wilson 1990). The peak at 933 cm^{-1} is specifically assigned to the C-O-C in α-1,4- linkage in the glycosidic chain of starch

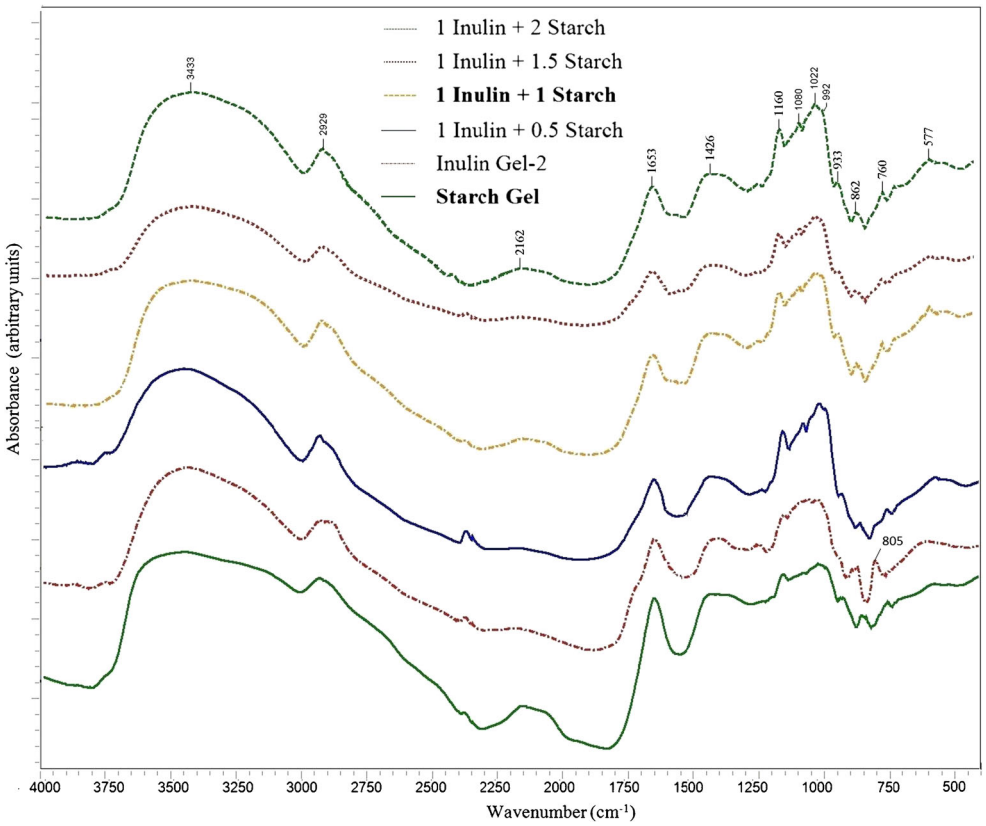

Fig. 1 FTIR spectra for models containing inulin and starch; Important bands: peaks below 800 cm^{-1}: skeletal vibrations of the fructose and glucose pyranose rings, 862 and 805 cm^{-1}: CH out-of -plane deformations of starch and inulin, 933 cm^{-1}: C-O-C in the glycosidic chain of starch, 1047 cm^{-1}: characteristic of crystalline starch, 1022 cm^{-1}: characteristic of amorphous starch, 1160 cm^{-1}: C-O-H and glycosidic linkages of the starch and inulin, 2929 and 1426 cm^{-1}: CH_2 stretching and bending vibrations in starch and inulin, 992, 1653 and 3433 cm^{-1}: hydrogen bonding of the hydroxyl groups

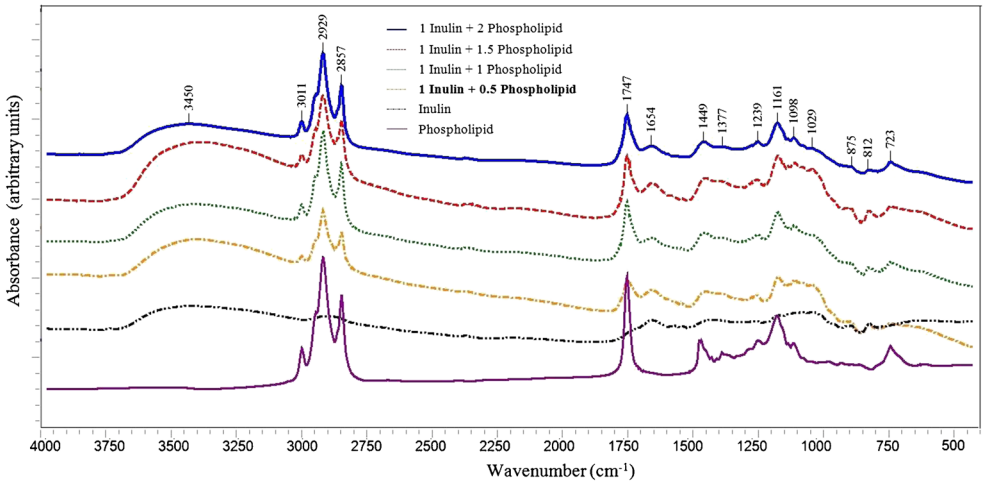

Fig. 2 FTIR spectra for models containing inulin and phospholipid; Important bands: 875 cm^{-1}: C-O-C stretching of the fructopyranose rings of inulin, 1747 cm^{-1}: C=O of phospholipids, 1449, 1377, 1161 and 723 cm^{-1}: C–H groups of phospholipids, 1098 cm^{-1}: phosphate group of phospholipids, 1239 cm^{-1}: Antisymmetric stretching of PO_2^- for phosphatidylcholine, 1098 and 812 cm^{-1}: alcohol group and symmetric stretching of PO_2^-, 3100–2750 cm^{-1}: stretch vibrations of C–H in the inulin and fatty acid moiety of lipids, 1654 cm^{-1}: OH bending of water, 3450 cm^{-1}: OH stretching of water

(Kačuráková and Mathlouthi 1996). Thus, the intensity of this peak was higher in the system models containing higher levels of starch. It was reported that the peak at 1047 cm^{-1} is characteristic of crystalline starch and the peak at 1022 cm^{-1} is characteristic of amorphous material (van Soest et al. 1995). As it could be seen from Fig. 1, intensity of peak 1022 cm^{-1} was increased with increasing the level of starch in the system. Also, absence of peak at 1047 cm^{-1} is probably due to gel formation during production of system models. The peak at 1160 cm^{-1} is assigned to the C-O-H and glycosidic linkages of the starch and inulin (Boussarsar et al. 2007). This intensity increment with increasing the levels of starch and inulin in the models confirms the enhancement of bond formation between them. It is exciting the presence of the peak at 1080 cm^{-1} in the models and absence of it in the inulin and starch spectra. This might be due to the bending vibrations of C-O-H linkages between starch and inulin (Boussarsar et al. 2007). The behaviour of the bands at 2929 and 1426 cm^{-1}, which are respectively assigned to CH_2 stretching and bending vibrations in starch and inulin, increase with addition level of them. Additionally, the peaks at 992, 1653 and 3433 cm^{-1}, which are related to hydrogen bonding of the hydroxyl group was reported to be sensitive to the level of water present (Bello-Pérez et al. 2005; van Soest et al. 1995). Higher levels of inulin and

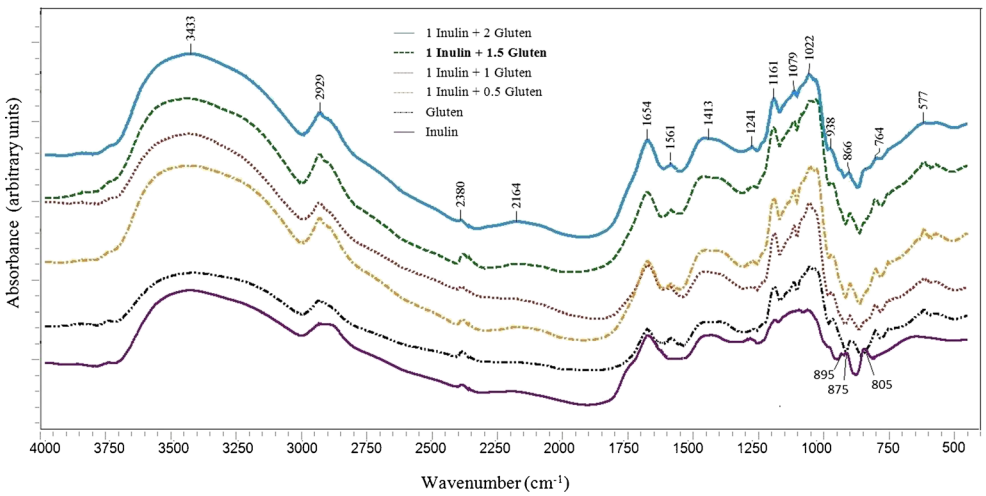

Fig. 3 FTIR spectra for models containing inulin and gluten; Important bands: peaks below 800 cm^{-1}: skeletal vibrations of the fructose and glucose pyranose rings, 866 cm^{-1}: stretching of C-O-C and out of plane bending modes of C-H in the gluten, 938 cm^{-1}: C-C stretching, N-H wagging and C-O-C vibrations of gluten, 1161, 1079 and 1022 cm^{-1}: C-O stretching mode of the C-OH groups of gluten and C-O groups of inulin, 1654 cm^{-1}: OH bending of water, 2929 cm^{-1}: C-H stretching of gluten and inulin, 3433 cm^{-1}: N-H stretching of gluten and OH stretching of water

starch resulted in the inducing of water entrapped in the model systems, which was consistent with the increased bands at these wavenumbers.

Inulin - phospholipid interaction

The IR spectra of Inulin - phospholipid mixtures are shown in Fig. 2. Main bands and their assignments according to the literature (Dreissig et al. 2009). The interval 1800–700 cm^{-1} is more useful to differentiate lipids because it constitutes a fingerprint for each component. In general, bands are assigned to the glycerol backbone of phospholipids, the hydrophilic head group and deformation vibrations of C–H groups of hydrophobic fatty acid chains. The vibration band observed at around 875 cm^{-1} is probably due to C-O-C stretching of the fructopyranose rings of inulin (Tsai 2007). The intensity enhancement of this bond is related to increase of inulin level in the system models. The IR spectrum of phospholipids contains bands due C=O (1747 cm^{-1}), C–H groups (1449, 1377, 1161 and 723 cm^{-1}) and the phosphate group (1098 cm^{-1}). The alcohol head groups attached to the phosphate group change the IR spectra. Antisymmetric stretch vibration bands of PO_2^- are visible at 1239 cm^{-1} for phosphatidylcholine (Dreissig et al. 2009). On the other hand, the positions of the symmetric stretch vibration bands of PO_2^- overlap with bands of the alcohol group to complex envelopes with main bands at 1098 and 812 cm^{-1}. Differences in band intensities correlate with the amount of lipid in the model, e.g., more intense bands at 1747, 1239, 1161, 1098, 1029 and 812 cm^{-1} in the IR spectrums indicate higher phospholipid content. In the interval 3100–2750 cm^{-1} bands originating from stretch vibrations of C–H groups dominate that are typical for the inulin and fatty acid moiety of lipids. Thus, addition of inulin and phospholipid in the model systems lead to the enhancement of intensity in this interval. On the other hand, increasing of water entrapped in the model systems is consistent with the increased bands at 1654 (OH bending) and 3450 cm^{-1} (OH stretching).

Inulin - gluten interaction

The FTIR absorbance spectra for the Inulin - gluten models are shown in Fig. 3. In the C-H stretching region between 2800 and 3000 cm^{-1}, a band at 2929 cm^{-1} is seen for all the models. The increase of gluten and inulin in the models led to the enhancement of the signals at this region, suggesting the important roles of model components levels in the interactions amongst them and consequently gluten network development (Haraszi et al. 2008). Stretch vibration band of N-H, which was visible at 3433 cm^{-1} for gluten, developed with gluten addition. On the other hand, the positions of the stretch vibration bands of N-H overlap with band of the OH stretching to complex envelopes with main bands at 3433 cm^{-1}. Increase of water entrapped in the model systems is consistent with the increased bands at 1654 (OH bending) and 3433 cm^{-1} (OH stretching). Small features at 2380 and 2164 cm^{-1} (which assigned as C–O stretching mode) remained unchanged in all of models. The absorption bands at 1241–1472 cm^{-1}, which are attributable to the C-O-O and C-N stretching and N-H bending (amide III) vibrations of gluten and inulin (Su et al. 2008), were possibly enhanced due to increase of model components. The bands at 1161, 1079 and 1022 cm^{-1} are due to the C-O stretching mode of the C-OH groups of gluten as well as the C-O groups of inulin (De Marchi et al. 2009; Parker 1971; Shen et al. 2010). The characteristic peaks below 938 cm^{-1} (C-C stretching, N-H wagging and C-O-C vibrations), were specially developed as a consequence of gluten addition (Pawlukojć et al. 2005). Also, the skeletal modes of the fructose rings of inulin lead to major bands at 760 and 577 cm^{-1} and minor bands between 577 and 400 cm^{-1} in the infrared spectra of samples (Kizil et al. 2002). The enhancement of intensity at this wavenumbers is related to increasing levels of gluten and inulin in models. It is also impressive that the peaks at 875 and 805 cm^{-1} was only observed in the spectrum of inulin. These peaks are probably due to out of plane bending modes of C-H in the fructopyranose units of inulin (Widjanarko et al. 2011). The absence of it might be due to completely mixing of inulin with gluten and subsequently elimination of indicated bending mode (Widjanarko et al. 2011). On the other hand, stretching vibrations of C-O-C and out of plane bending modes of C-H corresponding to the gluten were increased at 866 cm^{-1} (Sivam et al. 2013).

Typical gluten bands are Amide I (80 % C-O stretch, 10 % C-N stretch) at 1654 cm^{-1}, Amide II (60 % N-H bend, 30 % C-N stretch and 10 % C-C stretch) at 1561 cm^{-1} and Amide III (complex band resulting from several coordinate displacements) at 1413 and 1241 cm^{-1}. Peaks within the 1500–1800 cm^{-1} region are associated with Amide I and II signals of protein, carbonyl stretching modes of inulin and the O–H bending mode of water (Kačuráková and Mathlouthi 1996). This region of the spectra is examined in detail below using curve fitting routines.

Secondary structures

The potential usefulness of amide I spectra (1600–1700 cm^{-1}) for the determination of types of secondary structure quantitatively, as well as qualitatively, of proteins and smaller polypeptides in aqueous solution makes the accurate measurement of such spectra of great interest. The progress in the development of methods for analysis of spectral data makes it easier to distinguish the individual components within the intrinsically overlapped amide I band contours. Three analytic procedures in current use are Fourier self-deconvolution, second derivative, and band curve-fitting. The resultant protein spectra upon second-derivative analysis yielded bands with frequencies

characteristic of specific secondary structures that are essentially the same for all proteins. The second-derivative band areas (integrated intensities) gave relative amounts of different types of secondary structure for each protein that are nearly identical with the amounts computed from crystallographic data. It was concluded that amide I infrared spectra provide a simple and reliable method for the determination of the secondary structures of proteins and other polypeptides in aqueous solution (Bock and Damodaran 2012; Dong et al. 1990; Gorga et al. 1989). To analyze the structure of the gluten proteins contributing to the Amide I bands, curve fitting methods were applied to the original spectra of models over the region of 1600–1700 cm^{-1} (Fig. 4). All models had strong absorption bands at ~1654 cm^{-1}, which reflect α-helical structures (Wellner et al. 2003). The presence of α-helices is further proved by the presence of Amide II band found at ~1560 cm^{-1} (Naumann et al. 1993). The peak at ~1670 cm^{-1} in the spectra indicates the occurrence of β-turns which originated from the glutamine side chains (accounting for 35 % of the total amino acids in wheat protein) (Wellner et al. 2005). All spectra contained a peak at ~1633 cm^{-1} (assigned to intramolecular β-sheets), indicating intramolecular H bond interactions within proteins (Wellner et al. 2005). The absorptions at ~1629 and 1641 cm^{-1} likely resulted from the intermolecular β-sheets. As it could be seen in the curve fitted FTIR spectra of models (Fig. 5), β-turns were decreased from 22.45 to 20.98 % while α-helices increased from 23.12 to 26.97 %, when inulin to gluten ratio proportion of models increased. Upon Gaussian–Lorenzian curve fitting, the relative contribution of peaks characteristic of intermolecular β-sheets progressively increased whereas intramolecular β-sheets gradually decreased as the proportion of inulin in the models increased. The addition of inulin to models probably changed the amount of water bound to the gluten matrix. Although quantitative reasons for these changes are not clear, the results clearly indicate that inulin affects gluten-water interaction and redistributes the released water into other energy states (Sivam et al. 2012) as evidenced from a decrease in the intensity of the band at

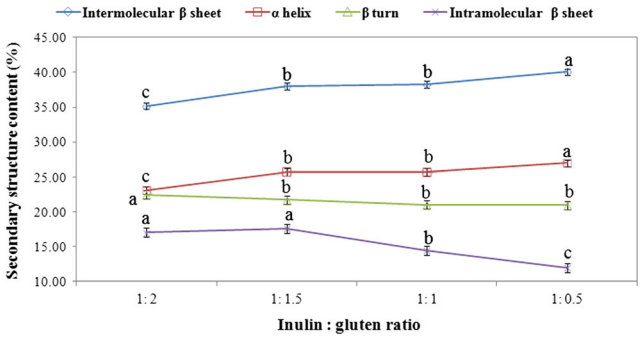

Fig. 5 Secondary structure content of models containing inulin and gluten; secondary structures were assigned via second derivative resolution enhancement and curve fitting with Gaussian–Lorenzian mix function for the amide I band region (1600–1700 cm^{-1}); Different letters represent statistically significant differences between treatments ($\alpha \leq 0.05$)

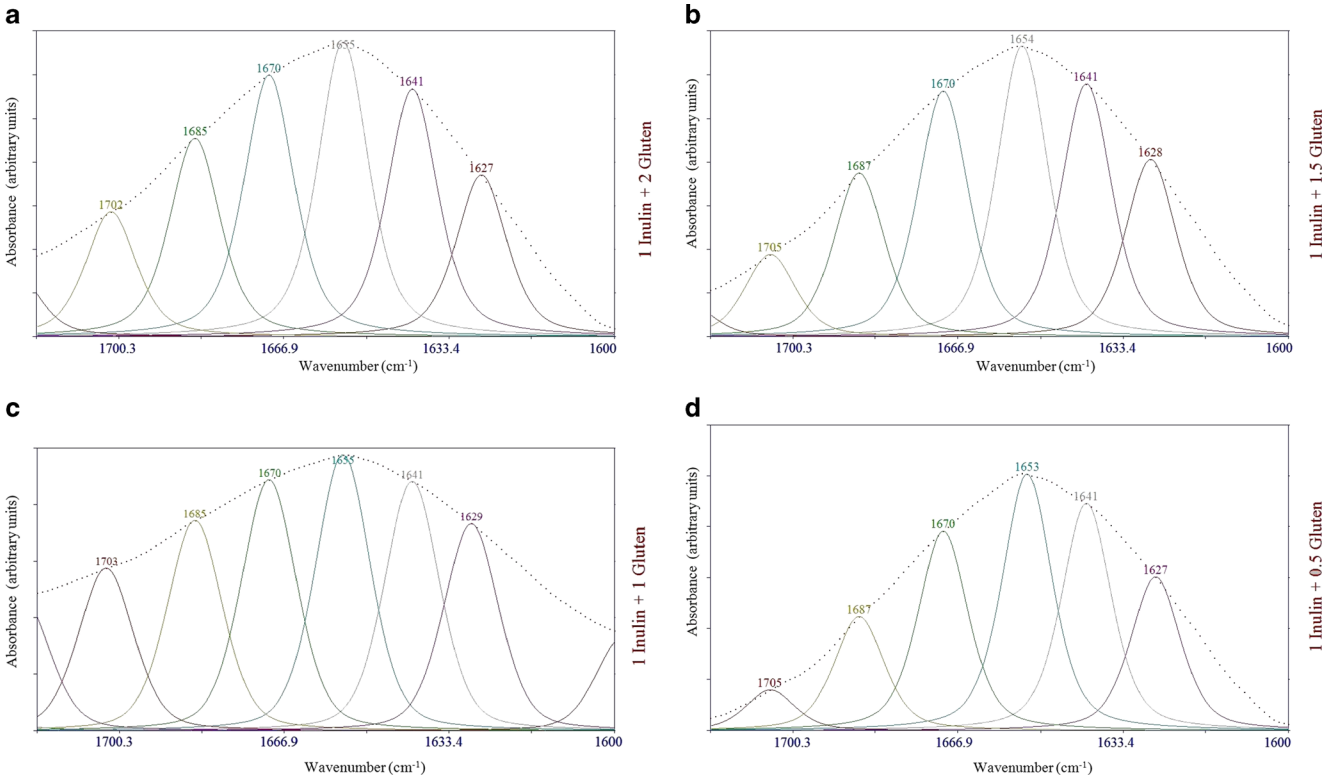

Fig. 4 Curve fitted FTIR spectra for models containing inulin and gluten; Gaussian–Lorenzian mix function was used for curve fitting of the amide I band region (1600–1700 cm^{-1})

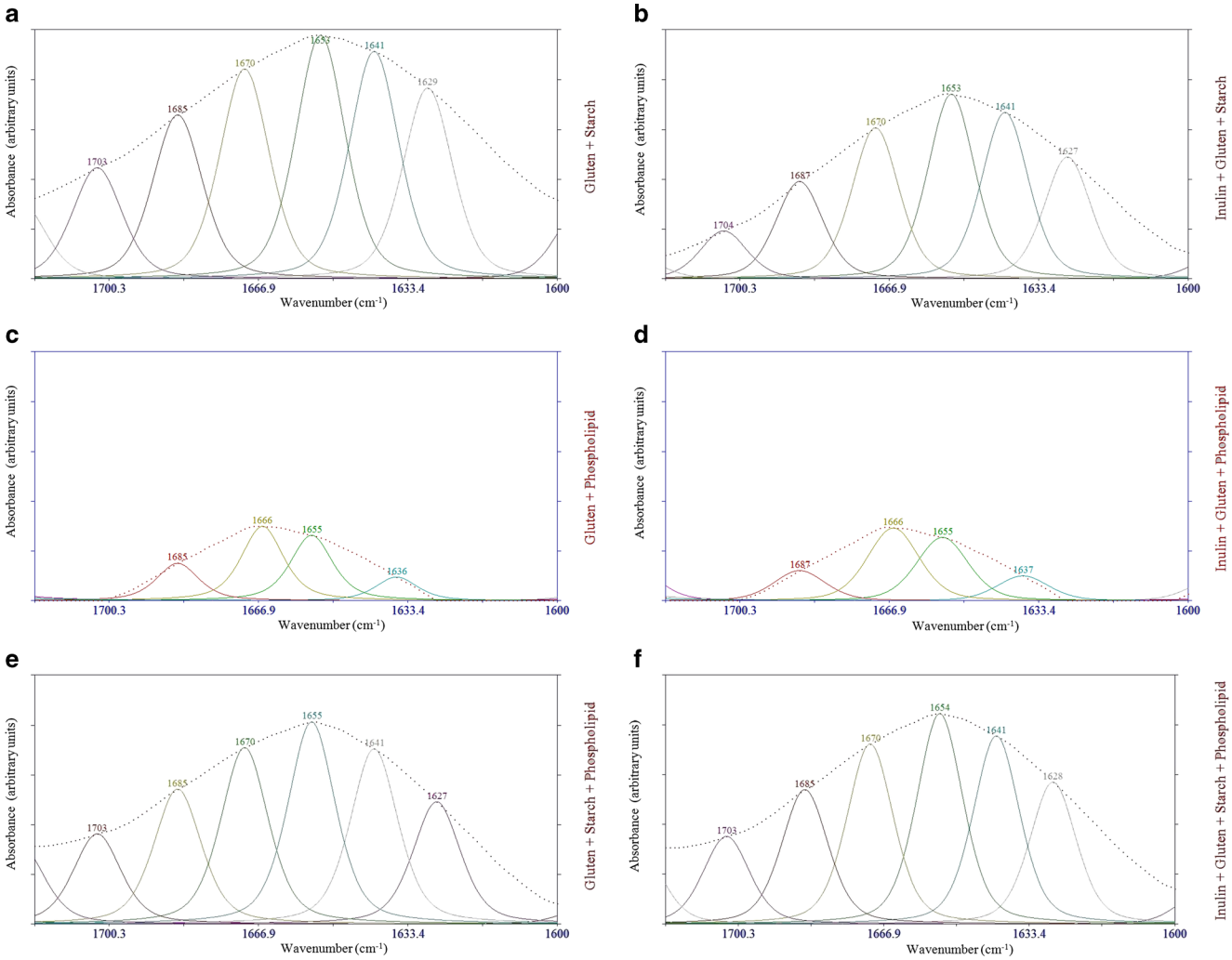

Fig. 6 Curve fitted FTIR spectra for models showing the effect of wheat biopolymers and inulin addition on the secondary structure of gluten; Gaussian–Lorenzian mix function was used for curve fitting of the amide I band region (1600–1700 cm^{-1})

3433 cm^{-1}. It seems to be a direct relation between trans-conformational changes in gluten and changes in the amount of gluten-water interaction in models as affected by inulin addition (Bock and Damodaran 2012). The β-turn structures in gluten might be related to the β-spiral domains in glutenin polypeptides (Wellner et al. 2005). These β-spiral structures can be regarded as consecutive β-turns. The β-spiral structures are implicated as one of the structural elements

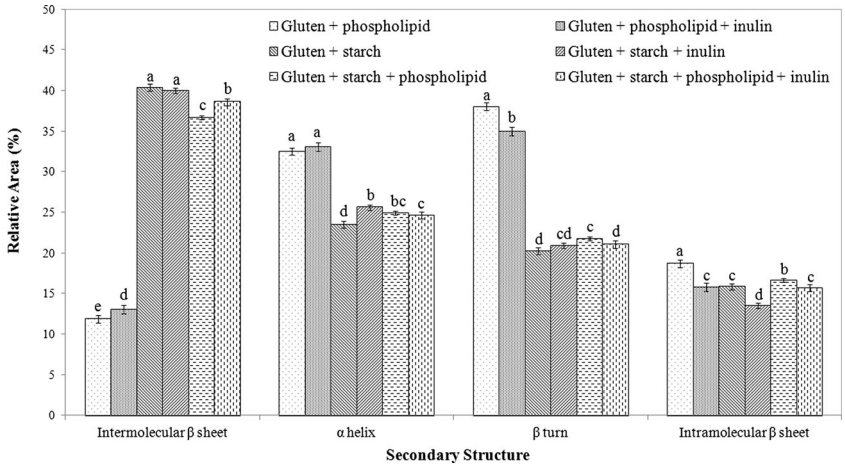

Fig. 7 Effect of wheat biopolymers and inulin addition on the relative areas and secondary structure of gluten; secondary structures were assigned via second derivative resolution enhancement and curve fitting with Gaussian–Lorenzian mix function for the amide I band region (1600–1700 cm^{-1}); Different letters represent statistically significant differences between treatments ($\alpha \leq 0.05$)

responsible for the viscoelasticity of dough (Wellner et al. 2005). The greater the amount of this structural element in dough, the greater would be the ability of dough to trap gas bubbles and the greater would be the bread loaf volume. Conversely, anything that transforms the β-spiral structure into intermolecular β-sheet structure would adversely influence the quality of breadcrumb (Bock and Damodaran 2012). Based on the results presented in this study, we hypothesize that one of the reasons for the adverse effect of inulin addition on loaf volume of bread (O'brien et al. 2003) is the collapse of the β-spiral structure to intermolecular β-sheets and this transformation is caused by redistribution of water in dough, which might involve in partial dehydration of gluten network. The loss of the elastic β-spiral structures and formation of inelastic intermolecular β-sheet aggregates in the gluten network might decrease the viscoelasticity of the dough and thus affect the loaf volume during bread making (Bock and Damodaran 2012).

It is also likely that in real wheat dough, interaction of other flour components, such as starch and phospholipid, might also modify the secondary structure of gluten. To test this speculation, the changes in the FT-IR spectra of the gluten, starch, phospholipid and inulin molecules were investigated when these components were mixed in the specified ratios. The curve fitting results for complex models are shown in Figs. 6 and 7. The intermolecular β-sheet, α-helix, β-turn and intramolecular β-sheet secondary structure contents of gluten in models, estimated from relative band areas in the spectral regions 1620–1640 cm^{-1}, 1650–1660 cm^{-1}, 1660–1680 cm^{-1}, and 1680–1695 $cm^{-1,}$ respectively (Mizutani et al. 2003; Sivam et al. 2012, 2013). As shown in the previous section, almost all of the β-turn and intramolecular β-sheet contents were decreased while intermolecular β-sheet and α-helix contents were increased by the addition of inulin to model systems. The intermolecular β-sheet and β-turn contents in the models of 17 and 18 which showing the interaction of gluten, starch and inulin were not significantly changed while the α-helix content of these models was only altered. It might be due to the fact that the starch molecules should interact with a part of the amino acid sequence which tends to fold into the α-helix (Mizutani et al. 2003). In addition, models of 19 and 20 that showing phospholipid and gluten interaction had the most β-turn, α-helix content and intramolecular β-sheet and the least intermolecular β-sheet content. The decrease in the intermolecular hydrogen-bonded β-sheets suggests that the phospholipid molecules penetrate the sites in which neighboring molecules tightly associate via β-sheets (Mizutani et al. 2003). It is well-known that the removal of phospholipid facilitates interactions amongst hydrophilic molecules. During breadmaking, oil modifies the surface properties of baking ingredients and influences CO_2 stability in dough (Sroan et al. 2009). When phospholipid is removed, water molecules move more freely and can more easily approach gluten, causing increased intermolecular β-sheets which in turn stabilizes β-turns (Sivam et al. 2012). In conclusion, phospholipids could be used to diminish the undesirable effects of inulin on the quality parameters of dough and bread.

Conclusion

The Fourier transform infrared spectroscopy is proved to be a valuable technique for studying interactions among Serish root inulin and bread components and secondary structure of gluten simultaneously in model systems. All the obtained information provides the insights into the differences in the conformations of models. The water redistribution in gluten dough by inulin addition alters the conformation of gluten from β-spiral (consecutive β-turns) structure to β-sheet structure. This major structural change in gluten might be the physical basis for poor quality of bread made with added inulin. This implicitly suggests that the adverse effects of inulin on bread quality could be overcome by decreasing the transformation of β-spiral structure into intermolecular β-sheet. However, since whole wheat dough is a complex system, it is quite possible that these components may also directly or indirectly affect gluten secondary structure as well as water distribution in the dough. This study was preliminary and another technique like circular dichroism spectroscopy is required to further identify the conformations.

Acknowledgments We would like to acknowledge Dr. Khashayarmanesh, and Mr Javad Ghazvini for their valuable help.

References

Aït Kaddour A, Barron C, Robert P, Cuq B (2008) Physico-chemical description of bread dough mixing using two-dimensional near-infrared correlation spectroscopy and moving-window two-dimensional correlation spectroscopy. J Cereal Sci 48:10–19

Bello-Pérez L, Ottenhof M-A, Agama-Acevedo E, Farhat I (2005) Effect of storage time on the retrogradation of banana starch extrudate. J Agric Food Chem 53:1081–1086

Bock JE, Damodaran S (2012) Bran-induced changes in water structure and gluten conformation in model gluten dough studied by Fourier transform infrared spectroscopy. Food Hydrocoll 31:146–155

Boussarsar H, Rogé B, Mathlouthi M (2007) Physico-chemical approach of the amylolytic action pattern of a thermostable amylopullulanase. Food Biophys 2:100–107

Byler DM, Susi H (1986) Examination of the secondary structure of proteins by deconvolved FTIR spectra. Biopolymers 25:469–487

De Marchi M et al (2009) Prediction of coagulation properties, titratable acidity, and pH of bovine milk using mid-infrared spectroscopy. J Dairy Sci 92:423–432

Dong A, Huang P, Caughey WS (1990) Protein secondary structures in water from second-derivative amide I infrared spectra. Biochem 29: 3303–3308

Dreissig I, Machill S, Salzer R, Krafft C (2009) Quantification of brain lipids by FTIR spectroscopy and partial least squares regression. Spectrochim Acta A Mol Biomol Spectrosc 71:2069–2075

Goodfellow B, Wilson R (1990) A Fourier transform IR study of the gelation of amylose and amylopectin. Biopolymers 30:1183–1189

Gorga JC, Dong A, Manning MC, Woody RW, Caughey WS, Strominger JL (1989) Comparison of the secondary structures of human class I and class II major histocompatibility complex antigens by Fourier transform infrared and circular dichroism spectroscopy. Proc Natl Acad Sci 86:2321–2325

Haraszi R, Larroque O, Butow B, Gale K, Bekes F (2008) Differential mixing action effects on functional properties and polymeric protein size distribution of wheat dough. J Cereal Sci 47:41–51

Kačuráková M, Mathlouthi M (1996) FTIR and laser-Raman spectra of oligosaccharides in water: characterization of the glycosidic bond. Carbohydr Res 284:145–157

Kizil R, Irudayaraj J, Seetharaman K (2002) Characterization of irradiated starches by using FT-Raman and FTIR spectroscopy. J Agric Food Chem 50:3912–3918

Mizutani Y, Matsumura Y, Imamura K, Nakanishi K, Mori T (2003) Effects of water activity and lipid addition on secondary structure of zein in powder systems. J Agric Food Chem 51:229–235

Mohamed A, Harry-O'Kuru RE, Gordon S, Palmquist DE (2009) Phospholipids and poly (glutamic acid)/hydrolysed gluten: Interaction and kinetics. Food Chem 114:1056–1062

Morris C, Morris GA (2012) The effect of inulin and fructo-oligosaccharide supplementation on the textural, rheological and sensory properties of bread and their role in weight management: a review. Food Chem 133:237–248

Naumann D, Schultz C, Goerne-Tschelnokow U, Hucho F (1993) Secondary structure and temperature behavior of the acetylcholine receptor by Fourier transform infrared spectroscopy. Biochemistry 32:3162–3168

Nikolic GS, Cakic MD (2007) Physical investigation of the colloidal iron-inulin complex. Colloid J 69:464–473

O'brien C, Mueller A, Scannell A, Arendt E (2003) Evaluation of the effects of fat replacers on the quality of wheat bread. J Food Eng 56: 265–267

Pal S, Mal D, Singh R (2005) Cationic starch: an effective flocculating agent. Carbohydr Polym 59:417–423

Panchev I, Delchev N, Kovacheva D, Slavov A (2011) Physicochemical characteristics of inulins obtained from Jerusalem artichoke (Helianthus tuberosus L.). Eur Food Res Technol 233:889–896

Parker FS (1971) Applications of infrared spectroscopy in biochemistry, biology, and medicine. Plenum, New York

Pawlukojć A, Leciejewicz J, Ramirez-Cuesta AJ, Nowicka-Scheibe J (2005) l-cysteine: neutron spectroscopy, Raman, IR and ab initio study. Spectrochim Acta A Mol Biomol Spectrosc 61:2474–2481. doi:10.1016/j.saa.2004.09.012

Peressini D, Sensidoni A (2009) Effect of soluble dietary fibre addition on rheological and breadmaking properties of wheat doughs. J Cereal Sci 49:190–201

Pourfarzad A, Habibi Najafi MB, Haddad Khodaparast MH, Hassanzadeh Khayyat M, Malekpour A (2014) Fractionation of eremurus spectabilis fructans by ethanol: box-behnken design and principal component analysis. Carbohydr Polym 106:374–383

Pourfarzad A, Habibi Najafi M, Haddad Khodaparast M, Hassanzadeh Khayyat M (2015a) Characterization of fructan extracted from eremurus spectabilis tubers: a comparative study on different technical conditions. J Food Sci Technol 52:2657–2667

Pourfarzad A, Habibi Najafi M, Haddad Khodaparast M, Hassanzadeh Khayyat M (2015b) Physicochemical properties of serish root (eremurus spectabilis) fructan as affected by drying methods. Qual Assur Saf Crops Food. doi:10.3920/QAS2014.0447

Roberfroid MB (1999) Nutritional and health benefits of inulin and oligofructose. Trials 129:1398S–1401S

Shen XL, Wu JM, Chen Y, Zhao G (2010) Antimicrobial and physical properties of sweet potato starch films incorporated with potassium sorbate or chitosan. Food Hydrocoll 24:285–290

Sivam A, Sun-Waterhouse D, Perera C, Waterhouse G (2012) Exploring the interactions between blackcurrant polyphenols, pectin and wheat biopolymers in model breads; a FTIR and HPLC investigation. Food Chem 131:802–810

Sivam AS, Sun-Waterhouse D, Perera CO, Waterhouse GIN (2013) Application of FT-IR and Raman spectroscopy for the study of biopolymers in breads fortified with fibre and polyphenols. Food Res Int 50:574–585

Sroan BS, Bean SR, MacRitchie F (2009) Mechanism of gas cell stabilization in bread making. I. The primary gluten–starch matrix. J Cereal Sci 49:32–40

Su JF, Huang Z, Yang CM, Yuan XY (2008) Properties of soy protein isolate/poly (vinyl alcohol) blend "green" films: compatibility, mechanical properties, and thermal stability. J Appl Polym Sci 110: 3706–3716

Tipson RS (1968) Infrared spectroscopy of carbohydrates: a review of the literature. US Department of Commerce, National Bureau of Standards

Tiwari U, Cummins E, Sullivan P, Flaherty J, Brunton N, Gallagher E (2011) Probabilistic methodology for assessing changes in the level and molecular weight of barley β-glucan during bread baking. Food Chem 124:1567–1576

Tsai CS (2007) Studies of Biomacromolecular Structures: Spectroscopic Analysis of Conformation. Biomacromolecules: Introduction to Structure, Function and Informatics. Wiley

van Soest JJ, Tournois H, de Wit D, Vliegenthart JF (1995) Short-range structure in (partially) crystalline potato starch determined with attenuated total reflectance Fourier-transform IR spectroscopy. Carbohydr Res 279:201–214

Vonhoff S, Condliffe J, Schiffter H (2010) Implementation of an FTIR calibration curve for fast and objective determination of changes in protein secondary structure during formulation development. J Pharm Biomed Anal 51:39–45

Wellner N, Bianchini D, Mills EC, Belton PS (2003) Effect of selected Hofmeister anions on the secondary structure and dynamics of wheat prolamins in gluten. Cereal Chem 80:596–600

Wellner N et al (2005) Changes in protein secondary structure during gluten deformation studied by dynamic Fourier transform infrared spectroscopy. Biomacromolecules 6:255–261

Widjanarko SB, Nugroho A, Estiasih T (2011) Functional interaction components of protein isolates and glucomannan in food bars by FTIR and SEM studies. Afr J Food Sci 5:12–21